

TRIUMF	UNIVERSITY OF ALBERTA EDMONTON, ALBERTA	
	Date 2000/06/30	File No. TRI-DNA-00-2
Author GM Stinson	Page 1 of 12	
Subject On the production of a hollow beam spot at the beam line 2A target		
<p><b>1. Introduction</b></p> <p>Beam line 2A at TRIUMF is designed to deliver 100 <math>\mu\text{A}</math> of 500 MeV protons to the target locations of the ISAC facility. Some years ago, it was suggested that the power density on a target at such beam currents could make it difficult to cool the target adequately. The question arose as to whether it was possible to sweep the beam in a circular motion at the target in order to distribute the heat load more evenly.</p> <p>Recently, it was noted that while steering the beam across the target higher yields were obtained when the beam had been steered close to the edges of the target<sup>1)</sup>. It is presumed that this was because reaction products produced near the target edges found it easier to diffuse out of the target than those produced in its interior. Consequently, the question of steering the beam around the periphery of the target arose again. In particular, the possibility of producing a hollow beam spot—a doughnut-shaped beam spot—at the target was raised again.</p> <p>This report presents a study of this latter question.</p> <p><b>2. Considerations in the production a hollow beam</b></p> <p>Beam line 2A was designed to produce a nominal beam size of <math>\pm 2.5</math> mm in each of the horizontal and vertical planes at the (existing) west target location. At the same time, the design specified a spatially achromatic beam spot (<math>R_{16} = 0</math>, <math>R_{26} \neq 0</math>) at the target. A detailed description of the optics of beam line 2A is given in ref<sup>2)</sup>.</p> <p>Existing targets of the ISAC facility have a diameter of approximately 18 mm. For this study it was decided to locate an AC <math>x</math>-<math>y</math> steering magnet 0.63 m upstream of the second 15° bending magnet of the beam line. The <math>x</math>- and <math>y</math>-windings would be powered 90° out of phase and their excitations would be adjusted such that the outer edge of the beam was approximately 9 mm from the target center.</p> <p>The SHIFT option of the program REVMOC<sup>3)</sup> was used to simulate the action of the steerer. This option applies specified impulsive shifts to any or all of the (geometric) phase-space coordinates. It was found that deflections of <math>\theta_{max} = 1.65</math> mr horizontally and <math>\phi_{max} = 2.15</math> mr vertically were required to provide the required horizontal and vertical deflections at the target center. These are illustrated in figures 1 and 2.</p> <p>Note: The REVMOC outputs shown in these figures (and the other distributions shown in this report) are two-dimensional (<math>x</math>-<math>y</math>) number distributions of the beam profiles calculated at the target center. For those unfamiliar with this output, the horizontal coordinates of beam particles in centimeters are obtained by reading down along the lower horizontal axis of each figure. Similarly, the vertical coordinates of beam particles, again in centimeters, are read along the left vertical axis. Numbers across the upper horizontal axis are the projections of the beam on the horizontal axis—that is, each number is the sum of all the numbers in a vertical column above a given horizontal position. Thus this is the horizontal distribution that one would expect to see read out from a wire chamber placed at the target center. In a similar manner, the numbers along the right vertical axis indicate the expected vertical distribution that would be seen there.</p> <p>Figures 1 and 2 were generated by including <i>only</i> scattering caused by the stripper foil. The effects of scattering caused by windows in the beam line was not included in these calculations. Figure 1 shows that</p>		

with a horizontal angular shift of 1.65 mr the horizontal beam centroid is shifted approximately 7 mm (from  $x = 0$  to  $x = 7.2$  mm). The outer edge of the beam then lies at the edge of the target ( $x \approx 9$  mm) and the inner edge ( $x \approx 5$  mm). Similar effects are shown in figure 2 in the shift in the vertical position of the beam when a 2.15 mr vertical shift is applied.

The effect of this (simulated) steering magnet was then obtained by setting its angular deflections,  $\Delta\theta$  (horizontal) and  $\Delta\phi$  (vertical), to

$$\left. \begin{aligned} \Delta\theta &= \theta_{max} \sin \alpha \\ \Delta\phi &= \phi_{max} \cos \alpha \end{aligned} \right\} 0 \leq \alpha \leq 350^\circ$$

with steps in  $\alpha$  of  $10^\circ$ . To conserve both computation time and computer memory, only 5,000 particles were traced at each value of  $\alpha$ . At the end of each individual run the computed coordinates of particles at the target center were output. When the complete angular range of  $\alpha$  had been completed, a final run was made in which the computed coordinates were used as input.

### 3. Foil-scattering only—an idealized case

The first runs were made with the inclusion of scattering in the stripper foil *only*. Thus any protective windows in the beam line were ignored. In this case it was found that no loss of particles due to scattering was predicted in any of the 36 individual runs. Thus the final run comprised a total of  $36 \times 5,000 = 180,000$  particles.

Figure 3 shows the predicted beam profile at the target center that results from the action of the steering magnet. It is important to remember that *only* scattering in the stripper foil has been taken into account in the production of this data. We consider a more realistic case in the next section.

However, from the results shown in figure 3 we may conclude that in principle it is feasible to produce an annular beam spot at the primary proton targets in beam line 2A. The idea of using an AC steering magnet to produce such a beam is, in fact, quite plausible.

### 4. A realistic beam line

While the results indicated in §3 above are valid for a beam line that does not have windows in the beam path, they are not a true representation of beam line 2A. This is because a 0.005 inch-thick aluminum window is located downstream of the last two quadrupoles of the beam line to isolate the beam-line vacuum from that of the target monolith. In addition there is a 0.010 inch-thick copper window at the entrance of the target vessel itself. Each of these windows will cause scattering of the incident primary proton beam. These effects are illustrated in figures 4 and 5.

Figure 4 shows the predicted beam profile at the center of the target when scattering in the stripper foil *only* is taken into account and *no* steering is applied. Figure 5 shows the predicted profile with scattering in the stripper foil *and* in the aluminum and copper windows included and, again, no steering applied. In each case a total of 150,000 particles was traced from the stripper foil to the target.

From figure 4 it is seen that virtually all of the beam is predicted to lie within the design goal of a beam spot diameter of 5 mm. A clean, well-defined beam spot is predicted if scattering could be limited only to that occurring in the stripper foil. On the other hand, figure 5 shows the effects of the aluminum and copper windows. The predicted beam spot is somewhat diffuse and a significant portion of the beam lies outside the design diameter. The additional scattering caused by the windows creates a significant beam halo. For all practical purposes, the beam diameter at the target center is 5 mm if only foil scattering is

taken into account. The beam size is roughly doubled when scattering in the aluminum and copper windows is also included. If we assume that the horizontal and vertical coordinates are independent, we can calculate the probability that beam particles lie outside a 5 mm diameter from the number distributions predicted in figure 5. From these we find that 4.8% of the particles have horizontal coordinates larger than  $\pm 2.55$  mm. Similarly, 7.7%, have their vertical coordinates larger than that value. We have

$$\begin{aligned} P(|x| > 2.55 \text{ mm and } |y| > 2.55 \text{ mm}) &= P(|x| > 2.55 \text{ mm}) + P(|y| > 2.55 \text{ mm}) \\ &\quad - P(|x| > 2.55 \text{ mm})P(|y| > 2.55 \text{ mm}) \\ &= 0.048 + 0.077 - 0.048(0.077) \\ &= 0.122 \end{aligned}$$

and thus some 12% of the beam is predicted to be scattered outside of the nominal beam size by the windows in the beam line. However, although not shown here, it is also predicted that virtually all of the beam is within the target diameter of 18 mm.

As noted above, figures 4 and 5 were produced by tracing 150,000 particles through the beam line. It was also noted that only 5,000 particles were traced for each run used to generate the coordinates of an annular beam. The upper portion of figure 6 shows the predicted beam spot when only 5,000 particles are traced through the beam line with stripper-foil scattering only. It is then equivalent to figure 4. Similarly, the lower portion of the figure shows the predicted beam spot with scattering in the stripper foil and in the windows included but with only 5,000 particles traced through the beam line. It is then equivalent to figure 5. Figure 6 is included in order to show that the predictions obtained when tracing a smaller number of particles do not differ significantly from those obtained when a much larger number of particles are traced. Indeed, if the number distributions from the lower portion of the figure are used and the above procedure to calculate the percentage of beam lying outside the nominal design diameter is followed, we obtain

$$\begin{aligned} P(|x| > 2.55 \text{ mm and } |y| > 2.55 \text{ mm}) &= 0.0486 + 0.0720 - 0.0486(0.0720) \\ &= 0.117, \end{aligned}$$

a value consistent with that calculated above.

The consequence of the additional scattering from the windows will be to increase the overall beam diameter at the target, and to fill in the hole in the beam that was shown in figure 3. This result is shown in figure 7. Although the full extents of the horizontal and vertical scales are the same ( $-1.24 \text{ cm} \leq x \text{ or } y \leq +1.24 \text{ cm}$ ), the minor divisions along the axes are different ( $\Delta y \approx 0.605 \text{ mm}$  and  $\Delta x = 0.8 \text{ mm}$ ). This is also true in figure 3 and has been done in order to make the physical extents of the horizontal and vertical scales the same, thus allowing a true representation of a circular spot to be portrayed.

Figure 7 was produced following the procedures outlined in §2 above except, in this instance, that the aluminum and copper windows were included in the calculation. From this figure it is immediately clear that the central hole of figure 3 has begun to fill in. Further, it is clear that a portion of the beam is predicted to lie outside the target diameter of 18 mm. Again assuming that the horizontal and vertical coordinates are independent and taking  $|x| \leq 0.92 \text{ cm}$  and  $|y| \leq 0.94 \text{ cm}$  as defining the outer extent of the target, we have

$$\begin{aligned} P(|x| > 9.2 \text{ mm and } |y| > 9.4 \text{ mm}) &= P(|x| > 9.2 \text{ mm}) + P(|y| > 9.4 \text{ mm}) \\ &\quad - P(|x| > 9.2 \text{ mm})P(|y| > 9.4 \text{ mm}) \\ &= 0.01856 + 0.00904 - 0.01856(0.00904) \\ &= 0.0274. \end{aligned}$$

Thus this study predicts that some 3% of the beam would be outside of the target dimensions. Roughly speaking, this fraction of the beam would be uniformly distributed around the target perimeter and would strike portions of the target support mechanism.

If the primary proton beam current were 100  $\mu\text{A}$ , the above implies a distributed spill of some 3  $\mu\text{A}$ . The question then arises as to whether such spills can be tolerated by the target support. Should this prove to be a problem, there are (at least) two solutions. The first would be to reduce the amount of steering. This would have the effect of more completely filling in the hole at the beam center. However, a majority of the beam would still remain relatively close to the perimeter of the target, thus providing a shorter diffusion path to its edge and, consequently, improving the collection of the radioactive species that are produced.

A second solution would be to increase the target diameter from 18 mm to, say, 24 mm. Then, if we assume that the particles in its four outer bins of figure 7—that is, the horizontal bins with 109 and 143 counts and the vertical bins with 129 and 90 counts—miss the target, the above procedure can be reapplied to obtain an estimate of how much beam strikes the target support mechanism. We have

$$\begin{aligned} P(|x| > 12 \text{ mm and } |y| > 12 \text{ mm}) &= P(|x| > 12 \text{ mm}) + P(|y| > 12 \text{ mm}) \\ &\quad - P(|x| > 12 \text{ mm})P(|y| > 12 \text{ mm}) \\ &= 0.00140 + 0.00122 - 0.0140(0.00122) \\ &= 0.00262. \end{aligned}$$

Thus, by increasing the target diameter by 30%, we have reduced the fraction of the beam missing the target by a factor of 10.

## 5. Discussion

This report has presented a study of the feasibility of producing a hollow beam at the target locations on beam line 2A. It has been shown that, in principle, this is possible. However, from a practical point of view, it has also been shown that the hole in the beam will be filled in because of scattering caused by the aluminum and copper windows upstream of the targets.

The scattering caused by the windows in the beam line will also produce an overall beam size that is larger than the (existing) targets. Should this cause problems, two possible solutions—an increase in the diameter of the target or a decrease in the amount of steering—have been presented. Section 4 gives some of the pros and cons of these possibilities.

It was also pointed out that to produce the results presented here different amounts of steering were required in the horizontal and vertical planes. This in itself is not a problem, but it is to be noted that the location of the steering elements in this study was not optimized. Rather, the steering was inserted in the first available space upstream of the targets. Consequently, should it be decided to attempt to produce a hollow beam on this beam line, the locations of the steering elements should be optimized.

As to the size of the steering elements that are required, a rough answer can be given. Because of the small deflection received by a particle in a steering magnet, we may ignore the difference between the arc length,  $s$ , along the trajectory of a particle that passes through a steerer and the straight-line effective length,  $L_{eff}$ , of the magnet. Then, if  $(B\rho)_0$  is the magnetic rigidity of a beam particle, and  $\rho$  and  $B$  the radius of curvature and the magnetic field, respectively, in the steering element, we have for an angular deflection  $\theta$

$$s = L_{eff} = \rho\theta = \frac{(B\rho)_0}{B}\theta = \frac{33.356p}{B}\theta$$

with  $p$  the particle momentum in  $\text{GeV}/c$ .

Because these steering magnets would be AC powered, their yokes would probably have to be laminated. Ignoring this or, equivalently, assuming that the driving frequency is sufficiently low that eddy current effects need not be considered, we can use the parameters of existing steering magnets at TRIUMF to get a size estimate. Thus, for the standard 4 inch steering magnets we have from measured data

$$L_{eff} = 9.87 \text{ inches} = 0.2507 \text{ m} \quad \text{and} \quad B_{max} = 1.5 \text{ kG.}$$

Thus such a magnet could deflect a 500 MeV proton through

$$\theta = \frac{0.2507(1.5)}{33.356(1.09007)} = 10.34 \text{ mr}$$

at full power. This is a factor of four larger than required. Similarly, the AECL  $x$ - $y$  steering magnets have a measured effective length of  $L_{eff} = 10.07$  inches (0.2558 m). Using this effective length and the measured fields, we tabulate below the predicted amounts of steering.

I (A)	3	3.5	4	4.5	5
B (kG)	0.27	0.31	0.36	0.40	0.44
$\theta$ (mr)	1.90	2.20	2.51	2.81	3.09

From tests at TRIUMF it is known that these steerers overheat if they are operated at 5 A DC for a period of over an hour. However, continuous operation at a current of 3 A DC causes no problem. Consequently, if these steerers are capable of continuous operation at 3.5 A DC, they would produce the required amount of steering.

From the above considerations we may conclude that the size of the required AC steering magnets would be similar to that of the standard 4-inch and the AECL steering magnets.

### References

1. P. Bricault, *Private communication*, TRIUMF, May, 2000.
2. G. M. Stinson, *Further revision of the optical design of beam line 2A*, TRI-DNA-98-2, TRIUMF, February, 1998.
3. C. Kost and P. Reeve, *REVMOC: A Monte Carlo Beam Transport Program*, TRI-DN-82-28, TRIUMF, 1982.

*Note added in proof.* As this note was being concluded, the author was made aware of two steering magnets that were used on the Van de Graaff that was at the University of Alberta. These are cylindrical  $x$ - $y$  steerers, constructed with laminated yokes and with sinusoidally distributed windings, that (nominally) operate at 20 Hertz. Their apertures are adequate for our purposes; their specifications are as follows.

Aperture diameter	3.04 inches	Maximum field	0.13 kG
Vacuum chamber clearance diameter	2.60 inches	Maximum power	15 V 3.5 A
Overall diameter	8.00 inches	Unipolar power supply	15 V 3.5 A
Overall length	11.65 inches	Bipolar power supply	$\pm 36$ V 5 A
Effective length	11.52 inches	Inductance	0.32 Henry

Based on these numbers and the above formalism, one of these steerers would produce a deflection of 1.07 mr. Consequently, two magnets in series would produce the required deflections. It is claimed that the field integral is constant to  $\pm 0.4\%$  over 95% of the clearance aperture (2.60 inches) and that the  $x$ -field strength at maximum setting is affected less than 2% by a zero to maximum variation of the  $y$ -field.





00/06/07 - 2A AT 500 MEV - Circular spot - NO Windows - 1.65 mr X + 2.15 mr Y

Distribution of particles INITIALLY ACCEPTED

Space # 2: Distribution of particles as a function of X AT TGTC (Element # 2) (along HORIZONTAL axis)  
& Y at TGTC (Element # 2) (along VERTICAL axis)  
COUNTS = 180000.

X PROJECTION

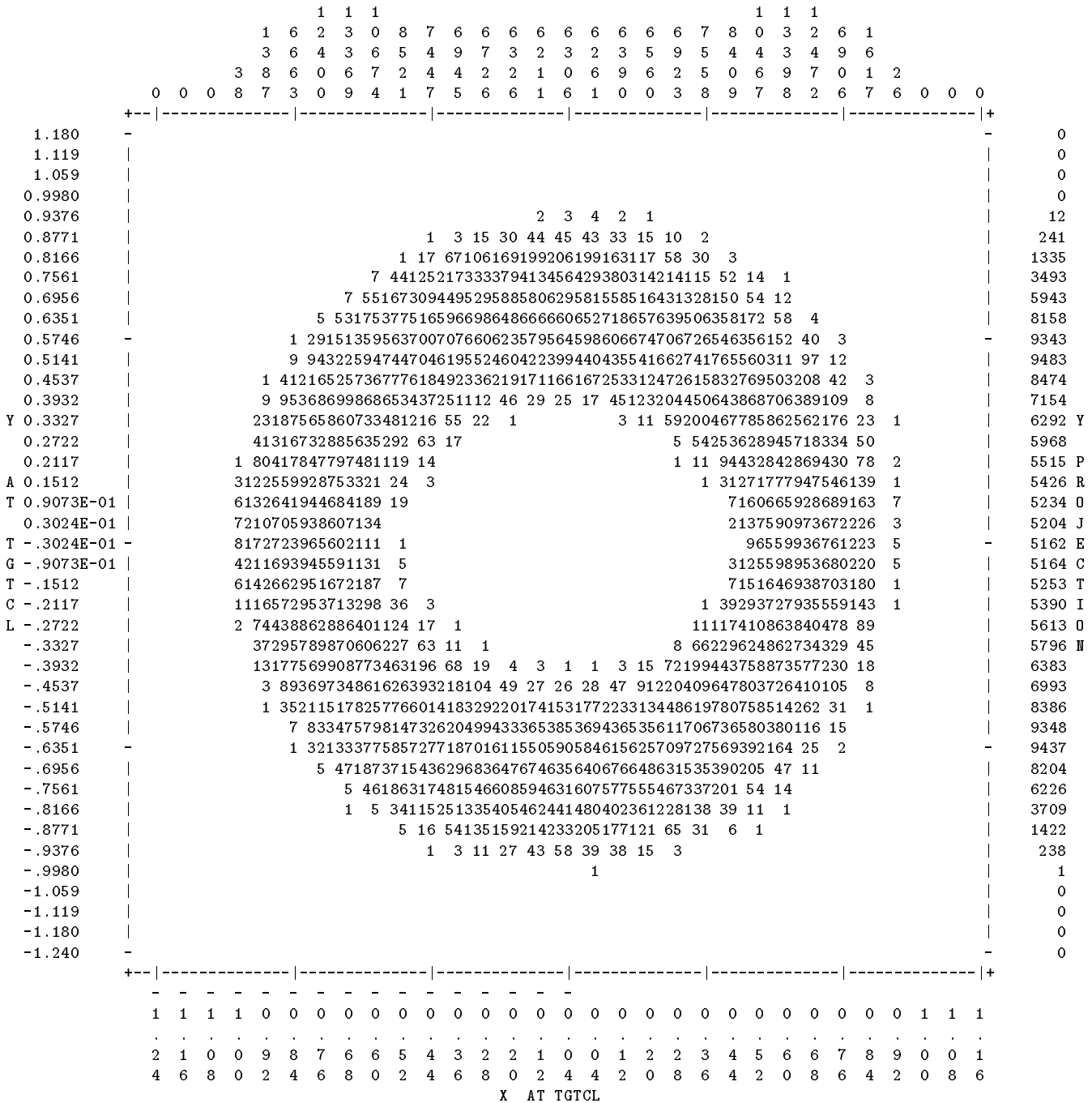


Fig. 3. The hollow beam predicted at the (west) target center by the steering magnet. Foil scattering Only is included.

00/06/07 - 2A AT 500 MEV - FINAL Leff - Stripper foil ONLY

REAL! Distribution of FINAL RUN FOUND HERE

Space # 4: Distribution of particles as a function of X AT TGTCL (Element #127) (along HORIZONTAL axis)  
& Y at TGTCL (Element #127) (along VERTICAL axis)

COUNTS = 149987.  
X PROJECTION

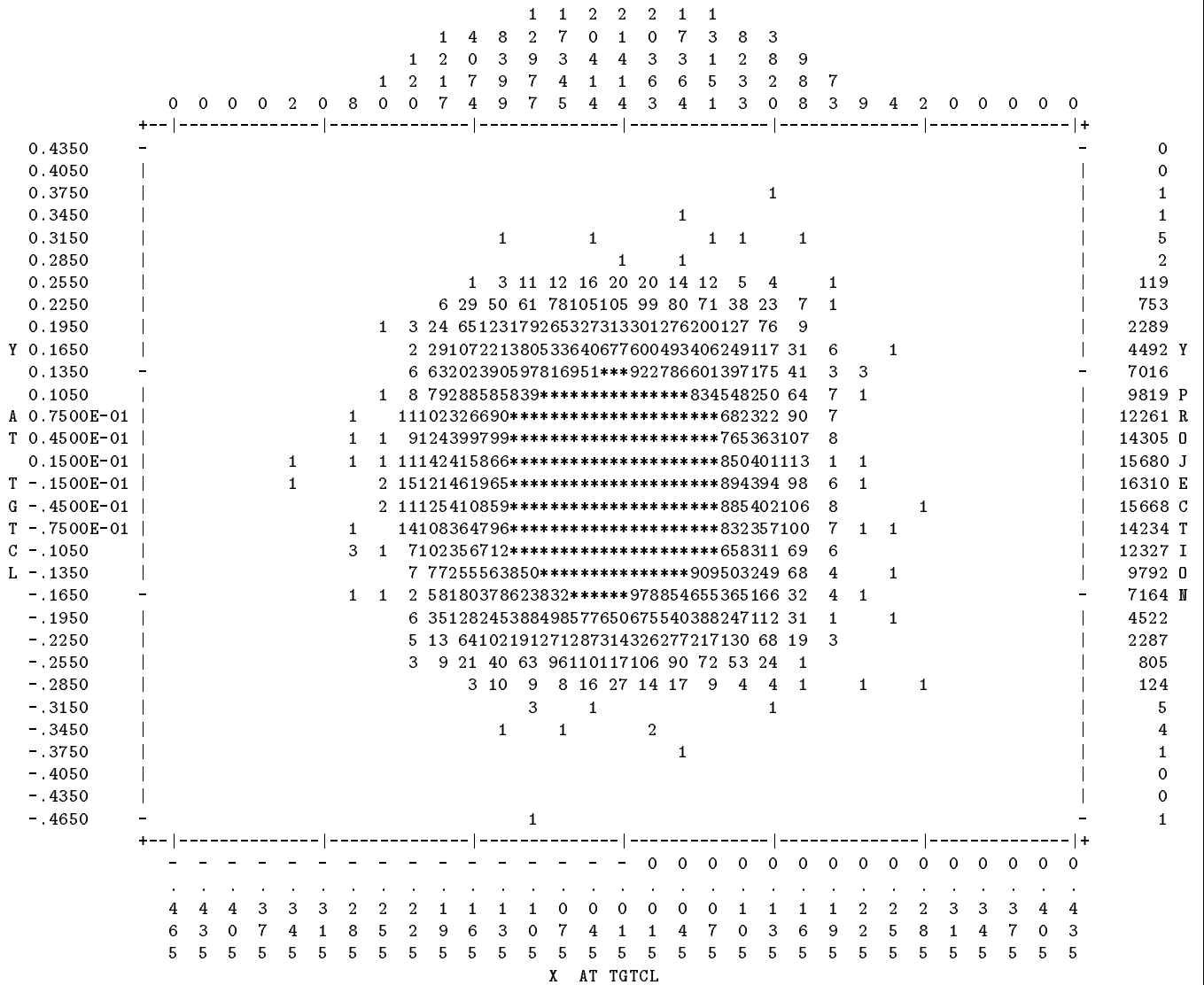


Fig. 4. The effect of the stripper foil on the beam spot at the target center of beam line 2A.

00/06/12 - 2A AT 500 MEV - FINAL Leff - 5Al+10Cu - NO Steering

REAL! Distribution of FINAL RUN FOUND HERE

Space # 4: Distribution of particles as a function of X AT TGTCL (Element #127) (along HORIZONTAL axis)
& Y at TGTCL (Element #127) (along VERTICAL axis)

COUNTS = 149629.

X PROJECTION

Table with 17 columns and 30 rows of particle counts. The columns are labeled with X coordinates from -39 to 47. The rows are labeled with Y coordinates from 0.4350 to -.4650. The table shows a distribution of counts that is roughly rectangular, centered around X=0 and Y=0.

Fig. 5. The effect of the stripper foil and of the 0.005 in. Al and 0.010 in. Cu windows on the beam spot at the target center of beam line 2A.



00/06/07 - 2A AT 500 MEV - Circular spot - .005 Al + .010 Cu Windows - 1.65 m

Distribution of particles INITIALLY ACCEPTED

Space # 1: Distribution of particles as a function of X AT TGTCL (Element # 2) (along HORIZONTAL axis)
& Y at TGTCL (Element # 2) (along VERTICAL axis)
COUNTS = 179498.

X PROJECTION

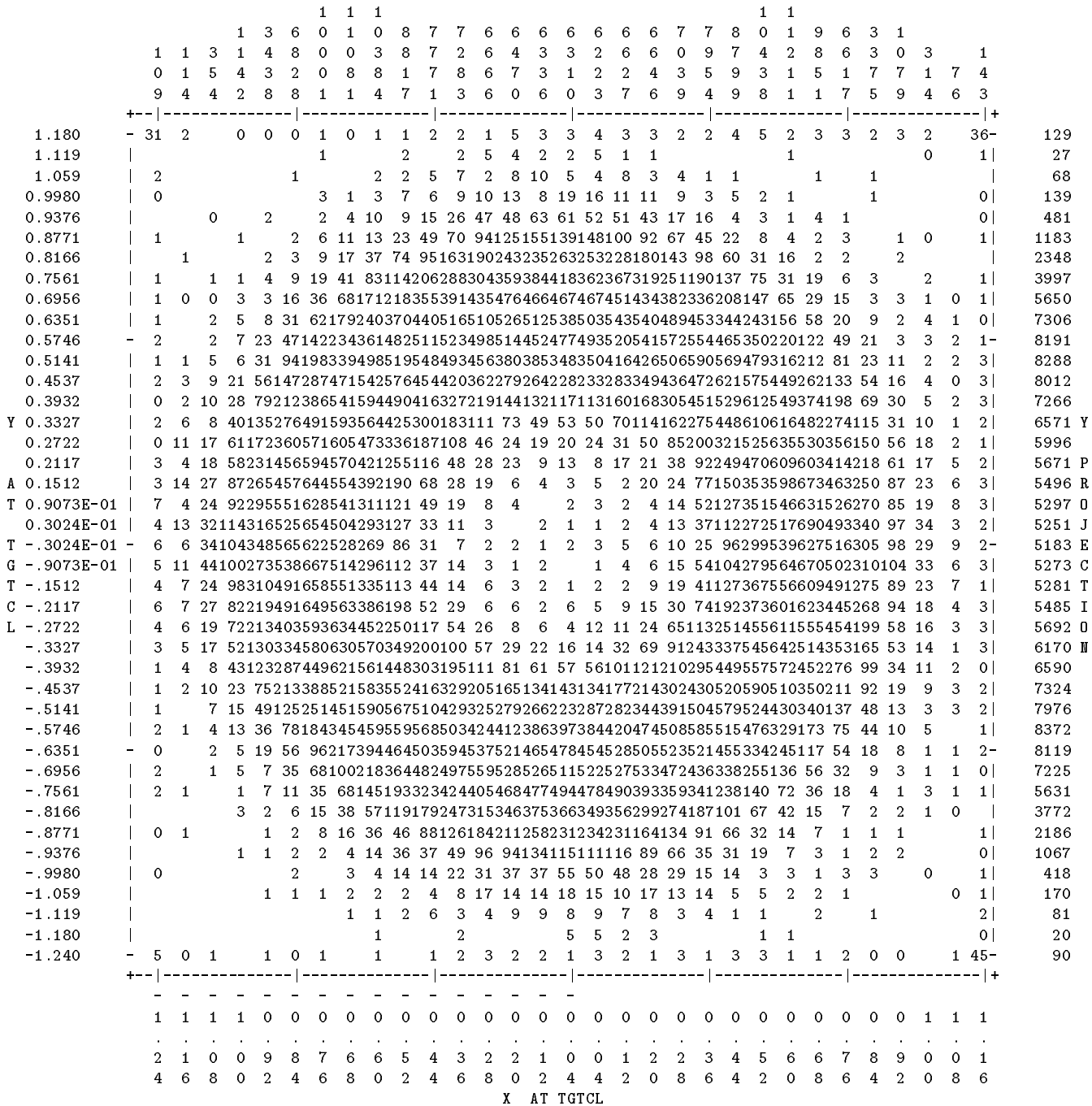


Fig. 7. The hollow beam spot predicted accounting for interactions in the stripper foil, the 0.005" Al isolation window, and the 0.010 Cu target window.